Scientia Iranica D (2016) 23(6), 2934–2943

Sharif University of Technology
Scientia Iranica
Transactions D: Computer Science & Engineering and Electrical Engineering
www.scientiairanica.com

Robust control of LVAD based on the sub-regional modeling of the heart

S. Ravanshadi[1] **and M. Jahed***

School of Electrical Engineering, Sharif University of Technology, Tehran, Iran.

Received 9 May 2016; accepted 13 August 2016

KEYWORDS
Ventricular assist device;
Adaptive robust control;
Distributed model;
Cardiovascular system.

Abstract. Left Ventricular Assist Devices (LVAD) have received renewed interest as a bridge-to-transplantation as well as a bridge-to-recovery device. Ironically, reports of malfunction and complications have hindered the growth of this device. In particular, the main concern is LVAD's susceptibility to excessive backlash and suction as a result of flows that are either too low or high, respectively. This study utilizes a well-established physiological model of the cardiovascular system as a reliable platform to study a proposed adaptive robust controller for a rotary motor based LVAD which overcomes such shortcomings. Proposed controller performance is evaluated by comparing simulated natural heart model with LVAD assisted diseased heart in various states, extending from 60 to 130 beats per minute (bpm). Simulation results of the proposed LVAD controller show that for heart rate of 75 bpm, systolic and diastolic blood pressures are 112 ± 18 mmHg and 73 ± 16 mmHg, respectively. Furthermore, for the light exercise condition of 130 bpm, systolic and diastolic blood pressures increase to 155 ± 19 mmHg and 96 ± 14 mmHg, respectively. These results closely match natural heart clinical measurements, confirming proposed LVAD model and its adaptive robust controller to be a possible solution to current issues confronting the LVAD drives.

1. Introduction

Left Ventricular Assist Device has been in operation since mid-1960s. In VAD implementation, unlike heart transplant and artificial heart, ventricles are kept in their entirety. The more recent rotary type of VADs introduced to clinical practice is becoming smaller and more efficient [1-5].

When a patient becomes more active, the cardiac activity exceeds its normal range and VAD operation must adjust to its specific physiologically dictated demand. One of the major deficiencies of VAD is its tendency to produce blood clots. As a result, there has been a major research interest with regard to their disturbance handling and detailed operation [6,7].

LVADs that are used in critical care settings are typically operated in open-loop fashion and are continuously supervised by a human operator in order to control such physiological parameters as blood pressure and heart beats. This type of control is heavily dependent on the operator; thereby, it could suffer from human errors. Certain VADs, such as Jarvik 2000 and DeBakey, work with constant speed. DeBakey operates by manually adjusting its speed to a perfusion comfort zone. This constant speed is sufficient for short-time usage of VAD; however, it is unsuitable for long-time usage [8]. In this work, a LVAD is utilized to assist the left ventricle in order to maintain required blood flow and pressure for systemic circulation [6,7,9,10].

One of the major problems of LVADs is associated with its motor speed and respective blood flow. When

1. *Present address: Electrical Engineering Department, Razi University, Kermanshah, Iran.*
*. *Corresponding author. Tel.: +98 21 66165937*
E-mail address: jahed@sharif.edu (M. Jahed)

rotary motor speed is too low, blood flow cannot be effectively pumped out of the heart and a backlash occurs in the respective ventricle. On the other hand, with higher rotational speeds, LVAD tries to pump more blood and may cause a phenomenon known as suction which results in collapse of the respective heart reservoir [11].

To prevent the suction action, VAD's operational speed must be adjusted. This control strategy is pertinent to specific pump and may cause overperfusion [12]. Due to the difficulty to detect the excessive perfusion and danger-of-suction region, efforts have been focused on suction avoidance algorithms. Chen et al. [13] showed that the gradient of LVAD flow in diastole reaches minimum with respect to pump speed when suction occurs. Other researchers studied the functionality of various controllers and compared their performances [14,15]. Parnis et al. [16] used a P controller for the Jarvik 2000 VAD. Rotational speed of the VAD was set as a linear function of the heart rate. Treadmill exercise and heart pacing studies were performed on a calf with the Jarvik 2000 VAD and no deleterious effects were detected during experiments. However, since the experiment was not extended to low and high flows, such a linear interpolation was not validated for an appropriate spectrum of LVAD operation. Waters et al. [17] designed a PI controller for an LVAD using pump head of LVAD as the feedback signal. In the study reported by Fu and Xu [18], the beating of the natural left ventricle was modeled as a sinusoidal disturbance to the LVAD, and a fuzzy controller was employed to regulate the LVAD flow to track a desired flow rate. The LVAD flow rate was estimated from the motor current and rotational speed, and the desired LVAD flow rate was assumed proportional to the heart rate. However, this assumption ignored the influence of heart contractility, and most importantly, the effect of the peripheral circulation on the desired flow rate.

Choi et al. [19] implemented a PI type fuzzy controller to realize a LVAD pump flow rate pulsatility tracking. A reference pulsatility signal of 15 mL/sec was selected to allow the natural heart to produce sufficient stroke volume while avoiding ventricular suction. The LVAD pump flow rate was estimated from the motor current and rotational speed. Simulation results showed that the control signal for this fuzzy controller produced a much smaller parameter variation in the LVAD speed than the PI controller. However, the constant setting of the reference pulsatility signal utilized in this study is questionable since patient's natural ventricle dynamism in a long-term period may dictate a different reference signal.

Giridharan and Skliar [20] designed an optimal controller with the structure of a PI controller to minimize some predefined penalty functions. The time-varying coefficients of the PI controller were obtained from offline, exhaustive numerical searches to minimize a weighting function, which was the combination of pump head or differential pressure between pulmonary vein and aorta and the variation rate of the rotational speed. However, it is not evident that dynamic and physical cardiovascular conditions can be adequately represented through such numerical practices; therefore, the optimality of this controller may not be guaranteed.

During the past decade, the $H\infty$ control scheme has been widely celebrated for its robustness in counteracting uncertainty perturbations and external disturbances [21,22]. As a consequence, such controllers were implemented for DC motors, switching converters, aircrafts, and PM synchronous motors [15,23,24].

A promising alternative to deal with perturbations and large parametric uncertainty is to use an adaptive control for which controller parameters are tuned as a function of some observed system variables. Motivated by this idea, it may be advantageous to synthesize a robust controller by considering parameter-tunable feedback law in order to achieve a prescribed $H\infty$-norm corresponding to some desired stability and tracking performance requirement.

Electromotor based LVAD modeled in this study has a nominal speed of 1450 rpm and power of 20 watts suitable for an acceptable range of cardiac output, namely 60, 75, 90, and 130 bpm [6,7,9,10,14,15]. Obviously, such a selection of cardiac output range is dictated by the nature of utilized rotary motor based LVAD device and operational expectancy of an LVAD assisted heart.

This study utilizes a robust adaptive controller for a rotational motor system under both parameter uncertainties and external load disturbance. We will illustrate that the proposed scheme is capable of tracking both step and sinusoidal commands and able to counteract external load disturbances. Here, step and sinusoidal commands resemble sudden and soft reference signals, respectively, issued to the LVAD controller. Since CV systems are inherently nonlinear, the derivation of the proposed controller rely on nonlinear $H\infty$ control theory. By choosing a quadratic storage function, the solution of the adaptive $H\infty$ problem is built on a simple structure, suitable for digital realization. To demonstrate the functionality of the adaptive controller, and thereby the parameter tuner in counteracting large parameter variations and external disturbance, the simulated results are provided with and without the parameter tuner of the adaptive $H\infty$ controller [25].

To verify the suitability of LVAD, one must integrate its model with an acceptable blood circulation model. Pressure-Volume (PV) models divide the circulation system into a series of elastic chambers and modules. Each elastic module models a

section such as the ventricle, atria, or aorta with uniquely described PV relationship [26]. Only a minimal number of parameters, such as chamber elasticity and arterial resistance, are required to create such models. Distributive PV models provide a detailed account of various functionalities of the CV system. The model drastically improves regional and behavioral accuracy based on subsystem modules by predicting inter-coupling variables and omitting unnecessary functionalities. The CV system being a collection of several organs and subsystems may then be collectively studied [27-29].

In the methodology section, initially, an electromechanical model of the CV system under normal condition is introduced. Next, the electromechanical model is expanded to include LVAD, followed by the derivation for the $H\infty$ controller. In the results section, the PV loop of the proposed LVAD system and controller simulation are provided. Finally, to verify the appropriate functionality of LVAD system, it is faired against corresponding simulated and clinical CV systems.

2. Methodology

2.1. Electromechanical model of the CV system

As a prerequisite to the controller study depicted in this work, an electrical distributed model is proposed to represent the functionality of the human CV system in a normal condition. The presented hydraulic electric analogy distributed model is arranged to model the vessels and organs of interest. Here R, L, and C represent physiological entities of vascular resistance, inertia of the blood, and vascular compliance, respectively. And, the model is formed through a series of single blocks, which ultimately represents the entire CV system. Both the single blocks and resulting distributed model of normal heart and CV system are introduced as an appendix at the end of this manuscript [24,25].

2.2. LVAD electromechanical model

LVAD pump is an electro-mechanical device that is driven by a rotary motor. The aim is to have the inertia load seated on the rotor shaft, closely track the specified motion speed. Figure 2 depicts the selected model for the LVAD, utilized in this work. Here, R_{iLVAD} is the input resistance of the pump, L_{iLVAD} input inertia of the pump, R_{oLVAD} output resistance of the pump, L_{oLVAD} output inertia of the pump, and $\text{R}_{\text{suction}}$ a resistance for suction. As evident, a linear model for the pump resistance is assumed throughout this study.

Furthermore, the LVADP block represents pump process and describes the relation between blood pressure, blood flow, and rotational speed of the motor as:

$$\Delta_P = bq + j\dot{q} + k\omega^2, \tag{1}$$

where Δ_P is the difference between input and output pressures of the pump, q is blood flow in the pump, ω is rotational speed of the pump and b, j, and k are the coefficients to be estimated. For the electromotor, the following relation between voltage variation and electrical current may be defined:

$$G_1(s) = \frac{I_a(s)}{\Delta V(s)} = \frac{1}{R_m + L_m s}, \tag{2}$$

where I_a is the motor current, $\Delta V(s)$ is electrical voltage differences between input and induction voltages of motor, R_m is electrical resistance of motor winding, and L_m is the electrical inductance of motor winding. A systemic depiction of relation between rotational speed and mechanical torque is given as:

$$H(s) = \frac{\Omega_m(s)}{T(s)} = \frac{1}{Js + B} = \frac{b}{s + a}, \tag{3}$$

where $\Omega_m(s)$ is the rotational speed in Laplace form of ω, T is the mechanical torque, B is a combination of damping coefficient and friction, J is the inertial component, and a and b are simply substituting B/J and $1/J$, respectively. The electromagnetic torque is given by:

$$T = K_t I_a. \tag{4}$$

For electromotor, a relation between rotational speed and input voltage is defined as:

$$G_M(s) = \frac{\Omega_m(s)}{V_i(s)} = \frac{K_t}{(R_m + L_m s)(Js + B) + K_t K_e}, \tag{5}$$

where $G_M(s)$ is transfer function of motor, $V_i(s)$ is electrical input voltage of motor, K_t is torque coefficient of the motor, and K_e is electrical coefficient of the motor [6,7,9,10,14,15,30].

2.3. H∞ controller derivation

Much like the approach given in [25], one needs to offset the variation in physical parameters and known disturbances through the usage of an adaptive control scheme. The proposed tracking controller utilizes an $H\infty$ approach as depicted in Figure 1.

The proposed scheme considers an appropriate feedback controller such that the closed loop system is internally stable. This approach is based on the robust adaptive control of the closed-loop transfer function.

To implement this scheme, the LVAD rotational speed problem must be formulated into an equivalent $H\infty$ control problem in which robust performance requirements are expressed in terms of $H\infty$-norm constraints on the tracking error dynamics. The dynamic

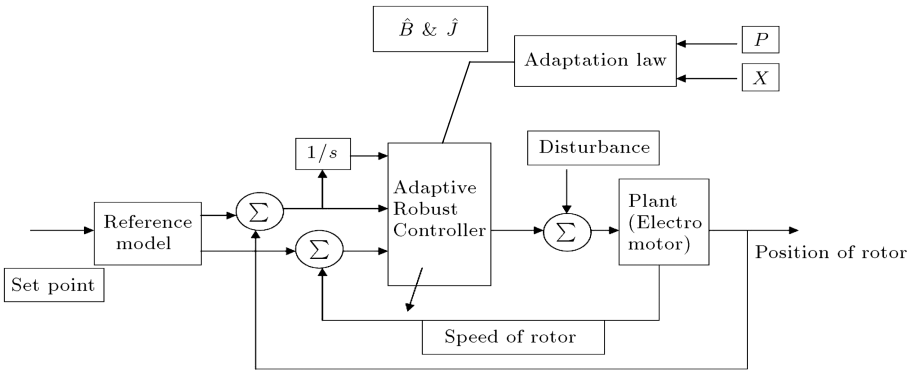

Figure 1. Block diagram of the proposed adaptive $H\infty$ ontrol scheme.

equation of the LPM drive system can be represented as:

$$\dot{\omega} = -\frac{B}{J}\omega + \frac{K_t}{J}v_i - \frac{1}{J}T_L, \tag{6}$$

where ω is the rotational speed of LVAD pump, and v_i is electrical input voltage of motor and represents an electrical voltage command. The tracking error vector is defined by:

$$E = [\theta - \theta_m, \omega - \omega_m]^T = [e, \dot{e}]^T, \tag{7}$$

where e is the tracking error of rotor angular position, θ_m and ω_m represent the desired rotor angular position and rotational speed, respectively. To establish the uncertainty of the plant parameters J and B, their estimates, namely $\hat{J}$ and $\hat{B}$, are introduced which suggest:

$$\Psi = [BJ]^T, \tag{8a}$$

$$\hat{\Psi} = [\hat{B}\hat{J}]^T, \tag{8b}$$

as their governing matrices. In order to obtain the dynamic tracking error for arbitrary input command, a preliminary feed-forward term is applied:

$$v_i = \frac{\hat{J}}{K_t}v + \frac{\hat{B}}{K_t}\omega + \frac{\hat{J}}{K_t}\dot{\omega}_m + \frac{\hat{J}}{K_t}[-K_e, E], \tag{9}$$

where $K_e = [k_1 k_2]$, k_1 and k_2 are arbitrary positive constants, and v is a loop control variable.

The rest of this work, including error dynamics, parameter-tunable controller, definition of the constraints, and proof of stability of the adaptive robust controller, has been fully discussed in [25,28-33].

2.4. LVAD integration in distributed CV model

Figure 2 represents the proposed functional model of the CV system integrated with the previously described LVAD model. To recall, LVAD is modeled through five elements, depicting blood viscosity and inertia, namely R_{iLVAD}, L_{iLVAD}, R_{oLVAD}, L_{oLVAD}, and R_{suction}, and one block representing the pump structure. The rest of the system is presented based on the previously introduced PV model and appropriate RLC parameter estimations per Recursive Least Square Algorithm (RLS).

3. Results and discussion

Simulation is carried out using responses for three cycles of step and sinusoidal position commands. Reference model is chosen as a third-order transfer function of the form [36]:

$$G_{\text{reference}} = \frac{13245}{s^3 + 84s^2 + 2315s + 13245}. \tag{10}$$

In the case of tracking sinusoidal trajectory, the reference model is set to a unit gain. Parameters used in the adaptive $H\infty$ design are given as:

$$Ke = [3\ 2], \quad d^2 = 0.2, \quad H = \begin{bmatrix} 0 & 0 & 0 \\ 0 & 11 & 0 \\ 0 & 0 & 0 \end{bmatrix}. \tag{11}$$

To solve the Riccati equation in [25], with a minimum value of γ, being 0.1211, P is given as:

$$P = \begin{bmatrix} 0.0832 & 0.0242 & 0.3268 \\ 0.0242 & 0.0001 & 0.0231 \\ 0.3268 & 0.0231 & 4.2561 \end{bmatrix} \times 10^5$$

$$\text{For} \quad \Gamma = \text{diag}\begin{bmatrix} 0.007 & 0.032 \end{bmatrix},$$

$$\Omega = \left\{ [\hat{B}\ \hat{J}]^T | 0 \le \hat{B} \le 2.8, 0.01 \le \hat{J} \le 0.9 \right\}.$$

Adaptive $H\infty$ controller is of the form:

$$\dot{\Theta} = -\Gamma\Phi B_2^T PX$$

$$= \begin{bmatrix} -(1.83e_1 + 0.07e_2 + 13.6\eta)\hat{J}^{-1}\dot{X} \\ -(7.4e_1 + 0.37e_2 + 58.03\eta)\hat{J}^{-1}\ddot{X} \end{bmatrix}, \tag{12}$$

and:

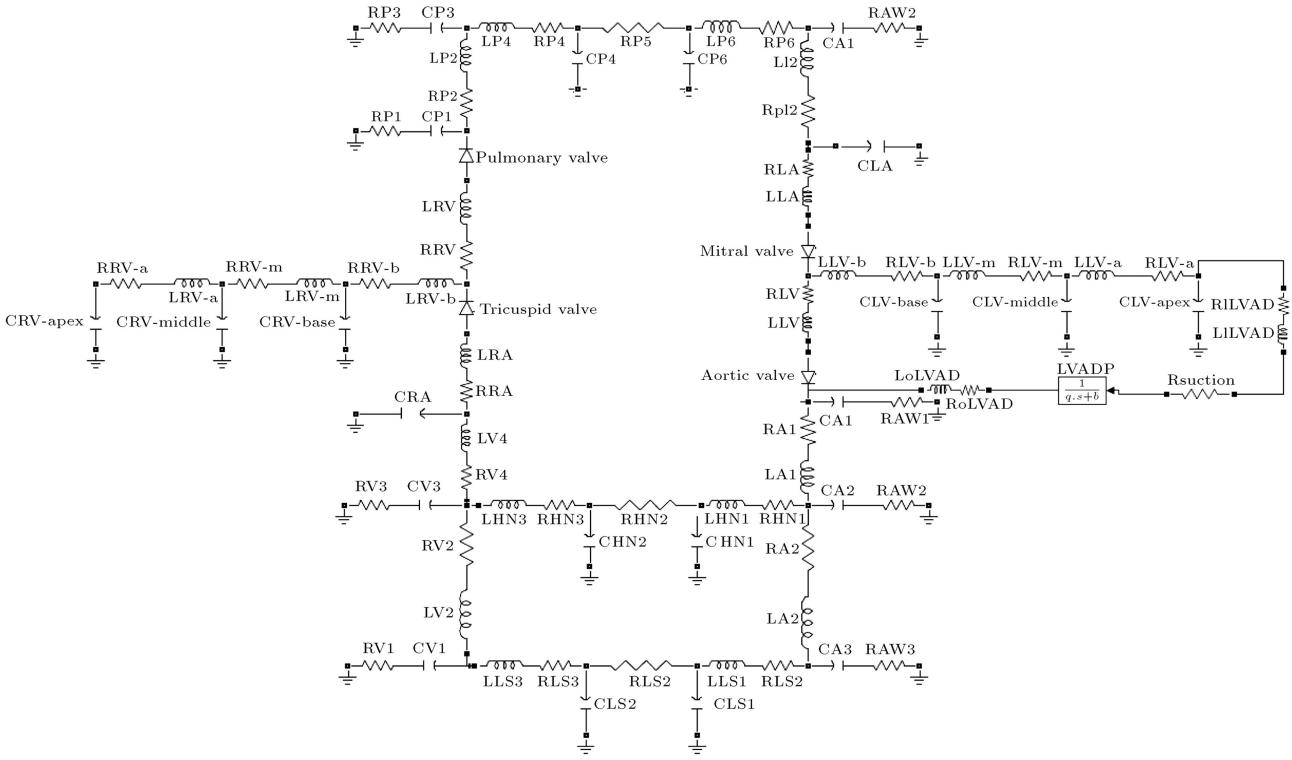

Figure 2. Circuit diagram of the distributed cardiovascular system with LVAD.

$$\dot{\hat{\Psi}} = \begin{bmatrix} \dot{\hat{B}} \\ \dot{\hat{J}} \end{bmatrix} = \begin{cases} \dot{\Theta} \text{ if } \hat{\Psi} \in \dot{\Omega} \text{ or } (\hat{\Psi} \in \delta\Omega \text{ and } \dot{\Theta}.N_{\hat{\Psi}} < 0) \\ 0 \text{ if } \hat{\Psi} \in \delta\Omega \text{ and } \dot{\Theta}.N_{\hat{\Psi}} > 0 \end{cases} \quad (13)$$

$$v = -\frac{1}{d^2} B_2^T P X = -2410e_1 - 108e_2 - 16200\eta. \quad (14)$$

To investigate the effectiveness of the proposed controllers, four cases resembling various physiological conditions, expressed as large parameter variations and external load disturbance on the shaft, are considered as follows:

- **Case I:** $J = \bar{J}, B = \bar{B}$, $T_L = 0$ where $\bar{J}, \bar{B}$ are nominal values of LVAD;
- **Case II:** Plant parameters are increased fourfold to evaluate the regularization of the plant under severe conditions: $J = 4\bar{J}, B = 4\bar{B}, T_L = 0$;
- **Case III:** Introduction of disturbance load in 3.5 seconds on a nominal based system:

  $J = \bar{J}, B = \bar{B}, T_L = 5$ Nm (in 3.5 seconds),

  where the nominal values of the motor are:

  $\bar{J} = 0.075$ N.m.s.rad/V, $\quad \bar{B} = 0.345$ Nm/V.

To demonstrate the usefulness of the parameter tuner in counteracting large parameter variations and external load disturbances, the condition with no active tuner is also presented. This is the case that the tuning parameters $\hat{J}$ and $\hat{B}$ of the feedback law in Eq. (9) are substituted by the fixed nominal parameters of the motor, namely $\bar{J}$ and $\bar{B}$ noted above. This controller will be referred to as the non-adaptive $H\infty$ controller.

The waveforms of the rotational speed for the non-adaptive and adaptive $H\infty$ control schemes in Cases I through III are depicted in Figure 3(Ia) through 3(IIIa) for step speed input, and Figure 3(Ic) through 3(IIIc) for sinusoidal speed input and their associated control efforts are depicted in Figures 3(Ib) through 3(IIIb) and 3(Id) through 3(IIId), respectively. It illustrates that rotational speed for the proposed adaptive system is soundly improved providing a rapid trace of the sinusoidal speed command. Furthermore, the control effort (motor current) is appropriately reduced for the proposed adaptive control.

In the proposed adaptive controller, the initial controller parameters are set to $\hat{J} = \bar{J}$ and $\hat{B} = \bar{B}$ for all the previously described cases. For the rotational speed step command, both non-adaptive and adaptive schemes yield zero steady-state tracking errors. This is due to the insertion of an integral action in the controller block. However, it can be seen that the transient performance of the non-adaptive $H\infty$ control system in Cases II and III (i.e., under parametric variation and external force disturbance) is inferior to the adaptive case. It is observed that the non-adaptive method requires a larger control effort. This clearly demonstrates the salient performance of the adaptive

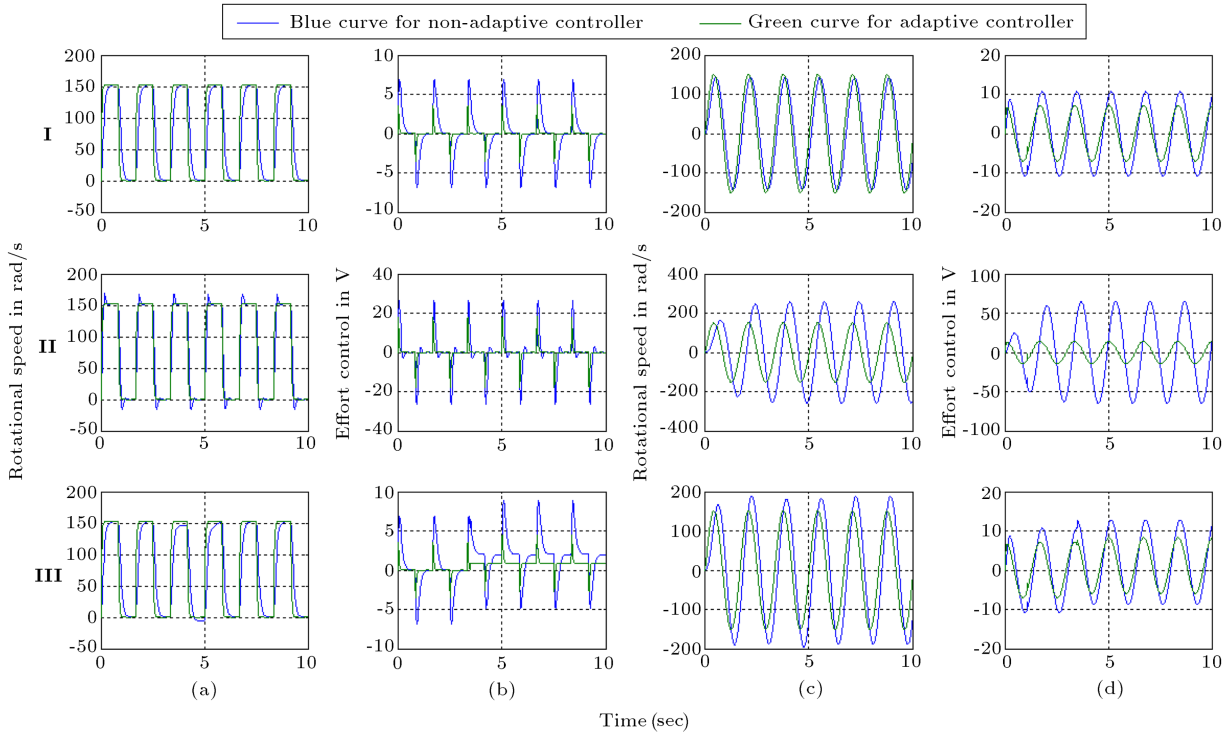

Figure 3. Comparing simulated results of non-adaptive and adaptive $H\infty$ controller for periodic step command: (Ia) Rotational speed of Case I; (IIa) rotational speed of Case II; (IIIa) rotational speed of Case III; (Ib) control effort of Case I; (IIb) Control effort of Case II; (IIIb) control effort of Case III. Comparing simulated results of Non-adaptive and adaptive $H\infty$ controller for periodic sinusoidal command: (Ic) Rotational speed of Case I; (IIc) rotational speed of Case II; (IIIc) rotational speed of Case III; (Id) control effort of Case I; (IId) control effort of case II; and (IIId) control effort of Case III.

$H\infty$ controller in both rotational speed command and external force regulation.

In view of Figure 3, there exists a tracking error during the transient and steady state in the non-adaptive case, for which the controller parameters $\hat{J}$ and $\hat{B}$ are fixed at their nominal values. However, in the adaptive case, the controller is able to tune $\hat{J}$ and $\hat{B}$ controller parameters, in effect, producing enough control effort to reduce the tracking error. Thus, Figures 3(IIIa) and 3(IIIc) clearly depict that the tracking error for the adaptive scheme is vanished. This demonstrates the effectiveness of the proposed adaptive scheme in counteracting large uncertainties and variations in the plant.

On the other hand, it is observed that the initial control efforts shown in Figures 3(Ib) through 3(IIIb) and 3(Id) through 3(IIId) are much less than those of the non-adaptive strategy. In tracking the sinusoidal waveform, a sudden change in command occurs at the start-up, which induces a large tracking error in rotational speed. This leads to a quite large initial control effort in the non-adaptive case as shown in Figures 3(Ib) through 3(IIIb) and 3(Id) through 3(IIId).

On the contrary, the adaptive controller does not give rise to such a demanding initial control effort. This is because, based on [25], the adaptation rates are related to both rotational speed error and its derivative, which can provide suitable tuning on the controller parameters $\hat{J}$ and $\hat{B}$; therefore, preventing the control effort from becoming unnecessarily large at the start-up. These results demonstrate that the proposed adaptive $H\infty$ control method performs much better than the non-adaptive scheme.

For clinical studies, patients were in a relaxed supine position. The range for age and weight of patients were 38 ± 14.5 years and 73.2 ± 15.7 kg, respectively. Six subjects ranging from the age of 42 to 64 years were asked to climb the treadmill. This information was further used as seeds for the simulation studies. The sampling interval for the simulation run was set at 0.5 ms.

To evaluate the operation of the LVAD system, the circulation model of Figure 2 was simulated for 10 normal subjects. Initially, using our previously introduced model, simulation was conducted for the normal CV system with a natural heart in place. In this model, in addition to the essential normal blood circulation parameters which include such parameters as left ventricle pressure and volume, CV parameters deduced from estimated RLC values were utilized [22].

Next, by substituting the LVAD for the natural heart model and utilizing RLC values for the vasculature per functional model of Figure 2, we were able to simulate the output parameters of interest. Figure 4(a)

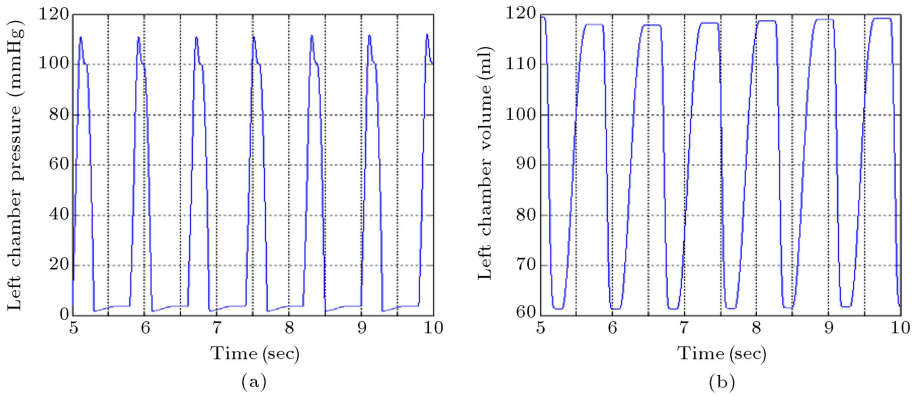

Figure 4. LVAD blood pressure (a) and volume (b) for the typical rest condition of 75 bpm.

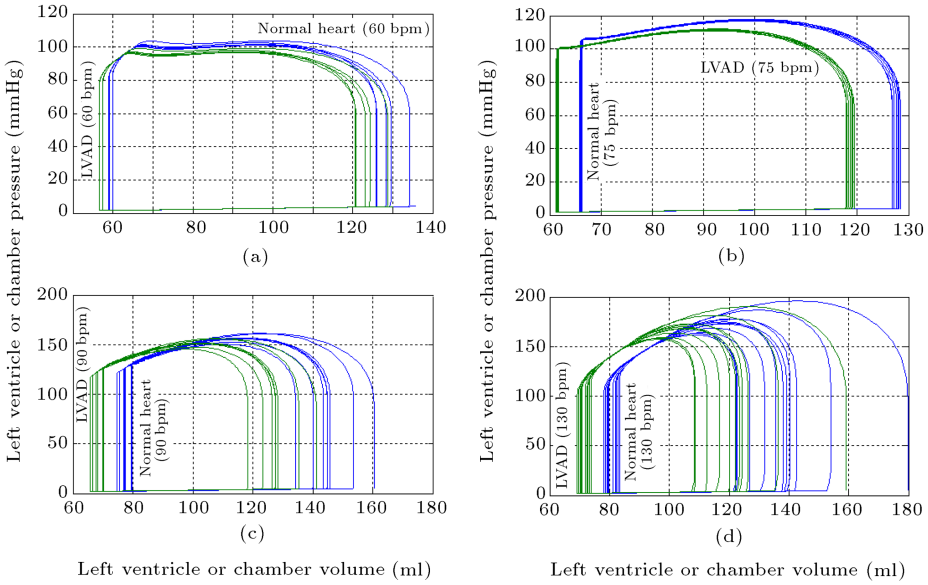

Figure 5. PV loop for normal LV (blue) vs. LVAD (green): (a) 60 bpm; (b) 75 bpm; (c) 90 bpm; and (d) 130 bpm.

and (b) depict typical blood pressure and volume for left ventricle with LVAD, respectively. In Figure 4(a), equivalent systolic and diastolic pressures were 4117 ± 15 mmHg and 72 ± 9 mmHg, respectively, where per Figure 4(b), equivalent diastolic blood volume is depicted as 118 ± 17 ml. Ejection Fraction (EF) deduced from these figures is measured at 65 ± 14 percent.

To compare natural heart functionality versus LVAD in normal physiological condition, Figure 5 depicts typical PV loops for 4 cases of lower limit rest to upper limit or light exercise (active load) conditions for normal versus LVAD heart. Specifically, Figures 5(a), (b), (c), and (d) show the PV loops for a lower limit rest condition of 60 bpm, normal rest state of 75 bpm, high end of rest condition at 90 bpm, and upper limit or light exercise state of 130 bpm, respectively.

Table 1 depicts the accumulated comparative results for clinical and simulated CV for natural heart, and adaptive $H\infty$ controlled LVAD for normal physiological condition. As shown, LVAD EF% is well within the acceptable range, attesting that LVAD has

Table 1. Accumulated results for clinical and simulated normal heart and LVAD.

	Clinical normal LV	**Simulated normal LV**	**LVAD**
# of patients	30	10	10 (simulation data)
Ejection fraction	71 ± 8 percent	73 ± 5 percent	65 ± 14 percent
Systolic blood pressure	122 ± 10 mmHg	118 ± 14 mmHg	117 ± 15 mmHg
Diastolic blood pressure	81 ± 13 mmHg	78 ± 15 mmHg	72 ± 9 mmHg

Table 2. Accumulated results for clinical and LVAD active load case of 130 bpm.

	Normal (clinical) in work position	LMTAH in work position
# of patients	10	10 (simulation data)
Heart beats	132 ± 11 bpm	130 bpm
Systolic blood pressure	147 ± 12 mmHg	155 ± 19 mmHg
Diastolic blood pressure	88 ± 10 mmHg	96 ± 14 mmHg

Table 3. Relation between rotational speed and LVAD equivalent bpm and cardiac output.

Rotational speed (rpm)	LVAD equivalent bpm	Cardiac output (lit/min)
1300	60	3.9
1450	75	4.7
1600	90	5.4
1950	130	6.6

successfully and effectively revived the functionality of the left ventricle.

To evaluate the operation of the LVAD system, the system was simulated for both normal and excessive loads. The load on the pump is increased when the patient is engaged in an excessive activity such as climbing the stairs or walking uphill. The subjects were asked to continue with the exercise for 10 minutes or until their diastolic pressure exceeds 100 mmHg. The resulting upper bound for their heart rates was averaged at 132 ± 11 (mean $\pm$ SD) bpm. Based on clinical data, LVAD systemic parameters were initially adjusted for a normal rate (motor pulse) of 75 beats per minute (bpm), increased to upper limit or active load case of 130 bpm.

As heart rate and vascular resistance are changed, systolic and diastolic blood pressures are varied accordingly. Such a variation causes systolic and diastolic blood pressures to increase to a maximum of 155 ± 19 and 96 ± 14 mmHg, respectively. Table 2 depicts the accumulated comparative results for clinical normal physiological condition and adaptive $H\infty$ controlled LVAD for active load cases. Table 3 describes the relation between rotational speed of electromotor and LVAD beat and CO of the CV system with LVAD in place. These parameters depict the operational relationship between mechanical speed and physiological state of interest.

4. Conclusion

Simulation of the proposed LVAD robust adaptive control shows flow behavior with less stress variation and recirculation, thereby suggesting reduction of the possibility of blood clot formation and reducing the risk of hemolysis and suction of the left ventricular reservoir. Unlike common $H\infty$ control design practices, the control scheme presented here introduced a feed-forward approach to achieve suitable tracking of sinusoidal and step commands. It was concluded that even under considerable parameter variations and external disturbances, the proposed adaptive robust control scheme improved the tracking performance when compared with non-adaptive robust design. With LVAD in place and as system load was increased from the 60 to 130 bpm, systolic and diastolic pressures and PV loops closely resembled similar simulated and measured values of the normal heart.

References

1. Canseco, D.C., Kimura, W., Garg, S., et. al. "Human ventricular unloading induces cardiomyocyte proliferation", *J. Am. Coll. Cardiol*, **65**(9), pp. 892-900 (2015).
2. Raymond, F., Estep, J.D., Agler, D.A., et al. "Echocardiography in the management of patients with left ventricular assist devices: Recommendations from the American society of echocardiography", *J. Am. Soc. Echocardiography*, **28**, pp. 853-909 (2015).
3. Mozafarian, D., Benjamin, E.J., Go, A.S., et al. "American heart association: heart disease and stroke statistics-2015 update", *AHA Statistical Update* (2015).
4. Pagani, F.D., Miller, L.W., Russell, S.D., et al. "Extended mechanical circulatory support with a continuous-flow rotary left ventricular assist device", *Journal of the American College of Cardiology*, **54**(4), pp. 312-321 (2009).
5. Miller, L., Pagani, F.D., Russell, S.D., et al. "Use of a continuous-flow device in patients awaiting heart transplantation", *New England J of Medicine*, **357**, pp. 885-896 (2007).
6. Wu, Z., Antaki, J.F., Burgreen, G.W., Butler, K.C., Thomas D.C. and Griffith, B.P. "Fluid dynamic characterization of operating conditions for continuous flow pumps", *ASAIO J*, **45**(5), pp. 442-449 (1999).
7. Boston, J.R., Simaan, M.A., Antaki J.F. and Yih-Choung Y. "Control issues in rotary heart assist devices", *Proc. American Control Conf.*, Chicago, IL, **5**, pp. 3473-3477 (2000).
8. Akimoto, T. "Rotary blood pump flow spontaneously increases during exercise under constant pump speed:

results of a chronic study", *Artificial Organs*, **23**(8), pp. 797-801 (1999).

9. Liu, D., Boston, J.R., Simaan M.A. and Antaki, J.F. "Multiobjective optimal control of a heart assist device", *Proc. 39th IEEE Conf. on Decision and Control*, Sydney, Australia, **5**, pp. 4857-4858 (2000).

10. Wu, Y., Allaire, P. and Tao, G. "An adaptive speed/flow controller for a continuous flow left ventricular assist device", *Proceedings of the American Control Conference*, Denver, CO, pp. 1171-1176 (2003).

11. Nakata, K., Ohtsuka, G., Yoshikawa, M., et al. "A new control method that estimates the backflow in a centrifugal pump", *Artificial Organs*, **23**(6), pp. 538-541 (1999).

12. Koeppen B.M. and Stanton, B.A. "Berne and Levy physiology", 6th Ed., Mosby Inc. (2010).

13. Chen, S., Antaki, J.F., Simaan, M.A. and Boston, J.R. "Physiological control of left ventricular assist devices based on gradient of flow", *Proc. IEEE American Control Conference*, Portland, OR, **6**, pp. 3829-3824 (2005).

14. Wu, Y., Allaire, P., Tao, G., et al. "An advanced physiological controller design for a left ventricular assist device to prevent left ventricular collapse", *Artificial Organs*, **27**, pp. 926-930 (2003).

15. Giridharan, G., Pantalos, G., Koenig, S., et al. "Achieving physiologic perfusion with ventricular assist devices: comparison of control strategies", *Proc. IEEE American Control Conference*, Portland, OR, USA, **6**, pp. 3823-3828 (2005).

16. Parnis, S.M., Conger, J.L., Fuqua, J.M. Jr., et al. "Progress in the development of a transcutaneously powered axial flow blood pump ventricular assist system", *ASAIO J*, **43**(5), M576-M580 (1997).

17. Waters, T., Allaire, P., Tao, G., et al. "Motor feedback physiological control for a continuous flow ventricular assist device", *Artificial Organs*, **23**(6), pp. 480-487 (1999).

18. Fu, M., Xu, L. "Computer simulation of sensorless fuzzy control of a rotary blood pump to assure normal physiology", *ASAIO J*, **46**(3), pp. 273-278 (2000).

19. Choi, S., Antaki, J.F., Boston J.R. and Thomas, D. "A sensorless approach to control of a turbodynamic left ventricular assist system", *IEEE Trans CST*, **9**(3), pp. 473-482 (2001).

20. Giridharan, G.A. and Skliar, M. "Control strategy for maintaining physiological perfusion with rotary blood pumps", *Artifial Organs*, **27**(7), pp. 639-48 (2003).

21. Jeong, D.Y., Kang, T., Dharmayanda, H.R. and Budiyono, A. "H-Infinity attitude control system design for a small-scale autonomous helicopter with nonlinear dynamics and uncertainties", *J of Aerospace Engineering*, **25**(4), pp. 501-518 (2012).

22. Bakule, A., Rehak, B., Papik, B. and Papik, M. "Decentralized H-infinity control of complex systems with delayed feedback", *Automatica*, **67**, pp. 127-131 (2016).

23. Brezina, L. and Brezina, T. "H-Infinity controller design for a DC motor model with uncertain parameters", *J of Engr. Mech.*, **18**(5/6), pp. 271-279 (2011).

24. Lee, T.S. and Chen, B.S. "Robust performance control of uncertain nonlinear systems: a self-tuning approach", *International J of Robust and Nonlinear Control*, **4**, pp. 697-712 (1994).

25. Ravanshadi S. and Jahed, M. "Introducing an adaptive robust controller for artificial heart", *Proc. IEEE BioRob Conference*, pp. 413-418 (2012).

26. Karamanoglu, M., Gallagher, D.E., Avolio, A.P. and O'Rourke, M.F. "Pressure wave propagation in a multibranched model of the human upper limb", *Am. J. Physiol*, **269**(4), pp. 1363-1369 (1995).

27. Ravanshadi S. and Jahed, M. "Introducing a distributed model of the heart", *Proc. of IEEE BioRob Conference*, pp. 419-424 (2012).

28. Ravanshadi S. and Jahed, M. "A novel distributed model of the heart under normal and congestive heart failure conditions", *Proc lMechE Part H: Journal of Engineering in Medicine*, **227**(4), pp. 362-372 (2013).

29. Snyder, M.F., Rideout, V.C. and Hillestad, R.J. "Computer modeling of the human systemic arterial tree", *J. Biomech.*, **1**(4), pp. 341-353 (1968).

30. Giridharan G.A., Skliar, M., Olsen D.B. and Pantalos, G. "Modeling and control of a brushless dc axial flow ventricular assist device", *ASAIO Journal*, **48**, pp. 272-289 (2002).

31. van der Schaft, A.J. "On a state space approach to nonlinear $H\infty$ control", *Sys. Contr. Lett*, **16**(1), pp. 1-8 (1991).

32. Fridman, E. "State feedback $H\infty$ control of nonlinear singularly perturbed systems", *International J. Robust and Nonlinear Control*, **11**(12), pp. 1115-1125 (2001).

33. van der Schaft, A.J. "L2-gain analysis of nonlinear systems and nonlinear state feedback $H\infty$ control", *IEEE Transactions on Automatic Control*, **37**(6), pp. 770-784 (1992).

34. Narendra K.S. and Annasawanny, A.M. *Stable Adaptive Systems*, New Jersey, Prentice-Hall (1989).

35. Gadewadikar, J., Lewis, F.L., Xie, L., Kucera, V. and AbuKhalaf, M. "Parameterization of all stabilizing $H\infty$ static state-feedback gains: application to output-feedback design", *Automatica (J of IFAC)*, **43**(9), pp. 1597-1604 (2007).

36. Xiao-wu, M., Xiao-li G. and Cheng, G.F. "Adaptive H-infinity control of a class of uncertain nonlinear systems", *Applied Mathematics and Mechanics*, **27**(9), pp. 1207-1215 (2006).

Biographies

Samin Ravanshadi received his BSc degree in EE from Mazandaran University, MSc and PhD degrees from Sharif University of Technology in 2000, 2004, and 2013, respectively. His research interests include modeling and control of physiological systems and prosthetic systems. Since 2015, he has been with Razi University in Kermanshah, Iran, as an Assistant Professor.

Mehran Jahed received his BSc in EE from Purdue University and Masters and PhD from University of Kentucky in 1982, 1987, and 1990, respectively. He was a Post-Doctoral fellow at Center for Excellence for Biomedical Engineering in University of Kentucky from 1990 to 1993. Since 1993, he has been a faculty member of EE department in Sharif University of Technology. His main areas of research include modeling and control, bio-robotics, and prosthetic systems.